CHAPTER 9

MONITORING INTERNAL COMBUSTION ENGINES BY NEURAL NETWORK BASED VIRTUAL SENSING

R.J. Howlett, **M.M. de Zoysa**, and **S.D. Walters**
Transfrontier Centre for Automotive Research (TCAR)
Engineering Research Centre, University of Brighton
Brighton, U.K.
R.J.Howlett@Brighton.ac.uk

Over the past two decades the manufacturers of internal-combustion engines that are used in motor vehicles have been very successful in reducing the harmful side effects of their products on the environment. However, they are under ever-increasing pressure to achieve further reductions in the quantities of polluting gases emitted by the engine, and a decrease in the amount of fuel consumed per kilometer. At the same time, vehicle characteristics that are desirable to the driver must not be compromised. Satisfying these diverse requirements requires precise engine control and comprehensive monitoring of the operational parameters of the power unit. Engines are highly price sensitive, and it is desirable to achieve the increased level of measurement that is required for enhanced control without additional sensory devices. Thus, the indirect estimation of quantities of interest using virtual-sensor techniques, without direct measurement using dedicated sensors, is a research area with considerable potential. Intelligent-systems techniques, such as neural networks, are attractive for application in this area because of their capabilities in pattern recognition, signal analysis and interpretation. For this reason, the use of neural networks in the monitoring and control of motor vehicle engines is an area of research which is receiving increasing attention from both the academic and commercial research communities. A virtual-sensor technique, the Virtual Lambda Sensor, is described here which uses a neural network for the estimation of air-fuel ratio in the engine.

1 Introduction

The internal-combustion engine is likely to be the most common motor-vehicle power plant until well into the twenty-first century, although new variants such as the Gasoline Direct Injection (GDI) and High Speed Direct Injection (HSDI) Diesel engines may supplant more conventional engine variants.

There are two recurrent themes in the area of automotive engine design: fuel economy and the reduction of harmful emissions from the exhaust. The emission of exhaust gases from Internal-Combustion (IC) engines is a major cause of environmental pollution. In addition the exhaust contains carbon dioxide, which is believed to contribute to the greenhouse effect and global warming. To reduce damage to the environment, governments in the United States, Europe, and parts of the rest of the world have introduced regulations that govern the permissible levels of pollutant gases in the exhaust. All manufacturers of motor-vehicles are required to undertake measures to ensure that their vehicles meet emission standards when they are new. In addition, the vehicle owner is required to ensure that the vehicle continues to meet in-service standards, by submitting it to periodic testing during routine maintenance. In the future, an on-board diagnostic system must be provided which carries out continuous monitoring.

Emission standards have been tightened progressively for over twenty years, to the point where emissions have been reduced by approximately an order of magnitude, measured on a per-vehicle basis. However, regulations are becoming even more stringent. Although existing methods of emission control are adequate to meet current regulations, they need improvements to enable them to meet future legislation [1]. The 1998 California Clean Air Act requires 10% of a manufacturer's fleet to be zero-emission vehicles (ZEVs), an 84% decrease in hydro-carbon (HC) emissions, a 64% decrease in oxides of nitrogen (NOx) output and a 60% reduction in carbon monoxide (CO) production for the entire fleet by the year 2003 [2].

On January 1, 1993, mandatory emission standards were introduced in Europe. This required all new petrol (gasoline) fueled vehicles in

Europe to be fitted with three-way auto-catalysts, thus bringing European standards to comparable levels with the US standards that had been introduced in the 1980s. In 1997, the second stage of regulations was brought into effect which covered both petrol and diesel vehicles. These regulations brought European standards into conformance with US standards up to 1996. The third stage of regulations, which sets standards for year 2000 and beyond, has been proposed. These regulations, when brought into effect, will require petrol-fueled vehicles with electronically controlled catalytic converters to be fitted with on-board diagnostic systems [1].

2 The Engine Management System

In order to achieve these standards it is necessary to maintain strict control of the operating parameters of the engine using a microprocessor-based Engine Management System (EMS) or Engine Control Unit (ECU). The EMS implements control strategies which aim to achieve optimum efficiency and high output power when required, while at the same time maintaining low emission levels. At the same time, in a spark-ignition engine, the EMS must operate the engine in a region favorable to the operation of a three-way catalytic converter, which further reduces the harmful content of the exhaust. The engine must also exhibit good transient response and other characteristics desirable to the operator, known among motor manufacturers as *driveability,* in response to movements of the driver's main control, the throttle or accelerator pedal. The EMS governs the amount of fuel admitted to the engine (via the fuel-pulse width), the point in the engine-cycle at which the mixture is ignited (the ignition timing), the amount of exhaust gas recirculated (EGR), and other parameters in advanced engine designs, for example, the valve timings. It determines values for these parameters from measured quantities such as speed, load torque, air mass flow rate, inlet-manifold pressure, temperatures at various points, and throttle-angle. Figure 1 illustrates the function of the EMS, which must essentially determine values for the *Controlled Variables* from a knowledge of *the Measured Variables*, in order to achieve the *System Aims*.

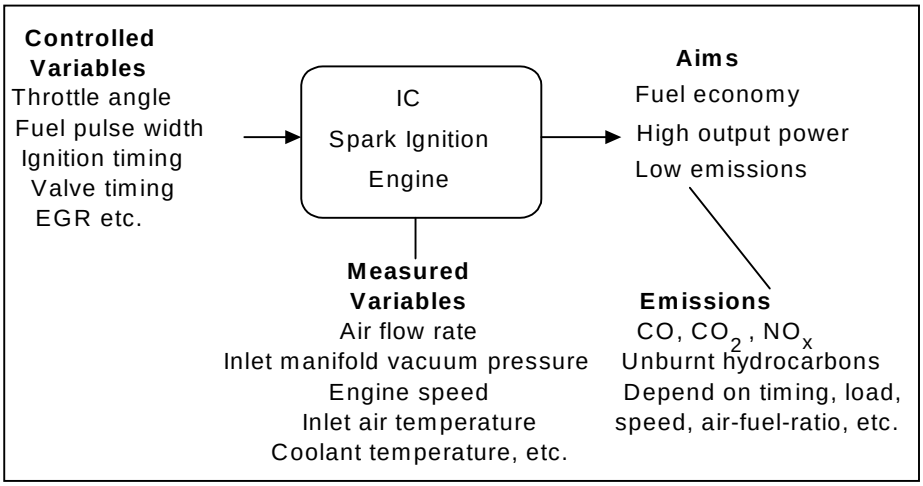

Figure 1. Internal combustion engine control.

The exact detail of the strategies which are used in commercial EMS products is a secret which is guarded closely by the manufacturers. One method which can be used for the selection of fuel pulse width and ignition timing values involves the use of *maps* which are look-up tables held in ROM. The EMS measures the engine speed using a sensor on the crankshaft and estimates the load, often indirectly from the inlet manifold (vacuum) pressure. These values are then used as indices for the look-up tables. Algorithmic and mathematical methods are also used. Research is taking place to develop improved engine control by incorporating neural networks and other intelligent-systems techniques into the EMS.

It has been mandatory in the US for some time, and now is also required in Europe, that, in addition to engine control, the EMS is required to perform *on-board diagnostic* (OBD) functions. Future OBD systems will be required to warn the driver, by means of a *malfunction indicator lamp* (MIL), of faults in the emission-control system which could lead to emission levels that are greater than those permitted.

The high level of accurate control necessary for engines to meet emissions standards requires that the EMS is supplied with comprehensive information about the operational parameters of the engine. Modern engines are equipped with a range of sensory devices which enables the measurement of quantities of interest. Speed,

manifold pressure, air mass flow rate, temperature at various points such as the air inlet are examples of quantities that are measured in many engines. In addition, parameters such as crank-angle and camshaft position are measured on more sophisticated power units. Accurate measurement of the ratio between the masses of injected petrol and air, known as the *air-fuel ratio*, is very valuable as an indicator of the point on its characteristics at which the engine is operating. Accurate air-fuel ratio measurement is difficult to achieve economically using conventional methods.

3 Virtual Sensor Systems

As engine control increases in sophistication the number of engine parameters which must be measured also increases. However, manufacturers are reluctant to install new sensors in the engine because of economic considerations. Engines are extremely price sensitive and additional sensors can only be economically justified if they provide very considerable improvements which could not be otherwise attained. Techniques which allow deductions to be made about quantities of interest without the installation of new sensors, by interpreting data from existing sensory devices in a new way, are especially valuable in this respect. The *virtual-sensor* technique allows an estimate to be made of a quantity of interest without the necessity for a sensor dedicated to the measurement. An example, which is described later in this chapter, is the Spark Voltage Characterization method of estimating the air-fuel ratio in the engine cylinder by analysis of the voltage signal at the spark plug.

Virtual-sensor systems require abilities in the domains of pattern-recognition, signal analysis and modeling. Neural networks have been shown to possess distinct strengths in these areas. For example, a neural network based virtual-sensor system is described in the literature that allows the prediction of emission levels from commonly measured quantities [3].

4 Air-Fuel Ratio

A parameter that is of considerable importance in determining the operating point of the engine, its output power and emission levels is the air-fuel ratio (AFR). The air-fuel ratio is often defined in terms of the *excess air factor*, or *lambda* ratio:

$$\text{lambda} = \text{AFR} / \text{AFR}_{st} \quad (1)$$

where AFR = the current air-fuel ratio
and AFR_{st} = the *stoichiometric* air-fuel ratio

Lambda is defined such that a lambda-ratio of unity corresponds to an air-fuel ratio of approximately 14.7:1 at normal temperature and pressure, when the fuel is petrol or gasoline. This is termed the *stoichiometric ratio*, and corresponds to the proportions of air and fuel which are required for complete combustion. A greater proportion of fuel gives a lambda-ratio of less than unity, termed a *rich* mixture, while a greater proportion of air gives a lambda-ratio of greater than unity, termed a *weak* or *lean* mixture. Maximum power is obtained when the lambda-ratio is approximately 0.9 and minimum fuel consumption occurs when the lambda-ratio is approximately 1.1.

Current engines reduce emission levels to within legislative limits by converting the exhaust gases into less toxic products using three-way catalytic converters. For optimum effect, three-way catalytic converters require that the lambda-ratio is closely maintained at the stoichiometric ratio (unity). In modern engines, a *lambda-sensor*, mounted in the exhaust stream, determines whether the lambda is above or below unity from the amount of oxygen present. The EMS uses this to adjust the fuel pulse width to keep the lambda-ratio approximately at unity. Power units currently under development, for example the gasoline direct injection (GDI) engine, may involve operation in lean-of-stoichiometric regions of the characteristics of the engine. Precise control of the air-fuel ratio is of considerable importance here also [4].

The lambda-sensor that is installed in most production vehicles has a voltage-lambda characteristic which effectively makes it a binary

device. It can be used to indicate whether the value of lambda is above or below unity, but it is unable to provide an accurate analogue measurement of air-fuel ratio. Accurate measurements can be made using what are referred to as *wideband* lambda-sensors, but they are very expensive, and in fact, even the currently used binary lambda-sensor represents an undesirable cost penalty.

The Spark Voltage Characterization method, described in detail later in this Chapter, allows the air-fuel ratio to be estimated from an analysis of the voltage signal at the spark plug, and so potentially offers the advantage that it permits the elimination of the lambda-sensor.

5 Combustion Monitoring Using the Spark Plug

Although it is not usually considered as a sensor, the spark plug is in direct contact with the combustion processes which are occurring in the cylinder. The use of the spark plug as a combustion sensor in spark ignition (SI) engines offers a number of advantages over other sensory methods. Many comparable techniques, such as pressure measurements or light emission recording by fiber-optics, require that the combustion chamber is modified; this can itself affect the combustion processes. Secondly, the price sensitivity of engines demands that the installation of a new sensor must result in very considerable improvements for it to be economically justifiable. The spark plug is already present in a spark ignition engine, eliminating the need to make any potentially detrimental modifications to the cylinder head, or combustion chamber, and avoiding additional costs which would result from the installation of new equipment. As the spark plug is in direct contact with the combustion, it is potentially an excellent observer of the combustion process. Analyzing the spark plug voltage (and possibly current) waveforms, therefore, potentially provides a robust and low-cost method for monitoring phenomena in the combustion chamber.

A method of using the spark plug as a combustion sensor which has received attention in the literature is known as the *Ionic-Current* method. This has been investigated for measuring combustion pressure, AFR and for the detection of fault conditions such as misfire and

knocking combustion. In the ionic-current system, the spark plug is used as a sensor during the non-firing part of the cycle. This is done by connecting a small bias voltage of about 100 volts to the spark plug and measuring the current. This current is due to the reactive ions in the flame which conduct current across the gap when the voltage is applied. The ions are formed during and after combustion, and the type and quantity of ions present depend on the combustion characteristics. The ionization current is also dependent on the pressure, temperature, etc. and therefore is rich in information but very complex [5]. Much work has been done on the use of ionic-currents for monitoring combustion, mainly to estimate combustion pressure, and so the method can act as a replacement for combustion-pressure sensors. Ionic-current systems have also been proposed for AFR and ignition-timing estimation, and misfire and knocking detection [6], [7]. More recently, neural networks have been applied to the analysis of ionic-current data for spark-advance control and AFR estimation [8], [9].

The ionic-current method appears attractive because only minor modifications are required to adapt the engine. However, high-voltage diodes or other switching methods are needed to isolate the ionic-current circuitry from the ignition system, when the high voltage is generated to initiate combustion. These have been prone to failure in the past. The 100V power supply is also an additional component which is required at additional expense.

A second spark plug based sensor technique, which is covered in depth in this chapter, is termed *Spark Voltage Characterization* (SVC). The SVC technique has a number of features in common with the ionic-current method. The SVC method involves the analysis of the time-varying voltage that appears across the spark plug, due to the ignition system, for monitoring combustion phenomena in the cylinder. This analysis can be carried out using a neural network. Using the spark plug as the combustion sensor, this technique has many of the advantages of the ionic-current method. However, as the SVC method involves analyzing the ignition voltage waveform itself, it eliminates the need for an additional bias power supply, and for the associated high-voltage switching circuitry. The use of SVC for estimating the in-cylinder air-fuel ratio is described later in this chapter.

6 The Ignition System of a Spark-Ignition Engine

Figure 2 shows the essential elements of an inductive-discharge ignition-system, as typically installed in a spark-ignition engine. The ignition-coil is essentially a high-voltage transformer, increasing the battery voltage (approximately 12V) to an extra high tension (EHT) pulse. This high voltage creates a spark between the contacts of the spark plug and initiates combustion. The contact-breaker was once a mechanical component in almost all engines, but in modern electronic ignition systems, it is replaced by a semiconductor switch such as an automotive specification transistor or thyristor.

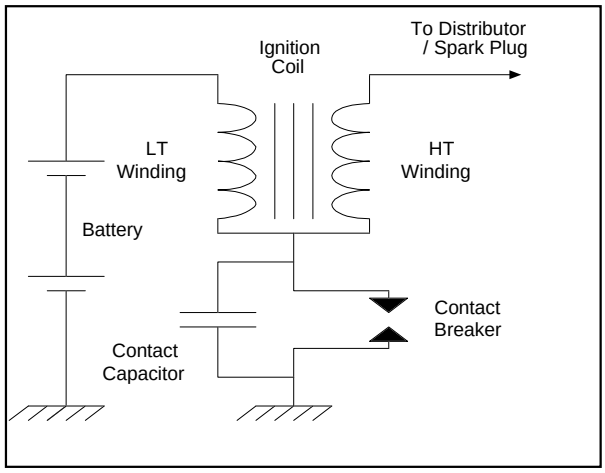

Figure 2. The ignition system.

The contact-breaker closes and current builds up in the low-tension (LT) winding of the coil resulting in the storage of energy; however, the speed at which this occurs is limited by the resistance of the coil. At an appropriate point in the engine-cycle, when an air-fuel mixture has been injected into the cylinder via the inlet-valve (in a port injection engine), and compressed so that the piston lies just before top-dead-center, the contact-breaker opens. The magnetic field in the coil collapses rapidly, with an equally rapid change in magnetic flux, and a high-voltage pulse is induced into the high-tension (HT) winding of the coil. A pulse of approximately 10kV appears across the spark plug terminals, igniting

the petrol-air mixture. The resulting combustion drives the power stroke of the engine.

Each cylinder in a four-stroke engine experiences one power stroke for every two revolutions of the crankshaft. In a multi-cylinder engine a mechanical switch geared to the crankshaft and known as a distributor is often used to switch the ignition-pulse to the correct cylinder. Alternative systems make use of multiple coils instead of a distributor. In a *dual-spark* or *wasted-spark* system each cylinder receives a spark once every crankshaft revolution instead of every 720 degrees of rotation. This requires multiple coils, in a multi-cylinder engine, but enables the distributor to be eliminated, and is common practice. Single-cylinder engines also commonly use this principle, as it allows the ignition system to be triggered directly from the crankshaft.

Figure 3 illustrates the spark-voltage waveform obtained from a typical ignition system. The spark plug voltage waveform has a number of predictable phases. As the EHT pulse is generated by the ignition-system the potential difference across the gap rises to between approximately six and 22 kV, before breakdown occurs. Breakdown is accompanied by a fall in voltage, giving a characteristic voltage spike of approximately 10 μs in duration. This is followed by a glow-discharge region of a few milliseconds duration, which appears as the tail of the waveform.

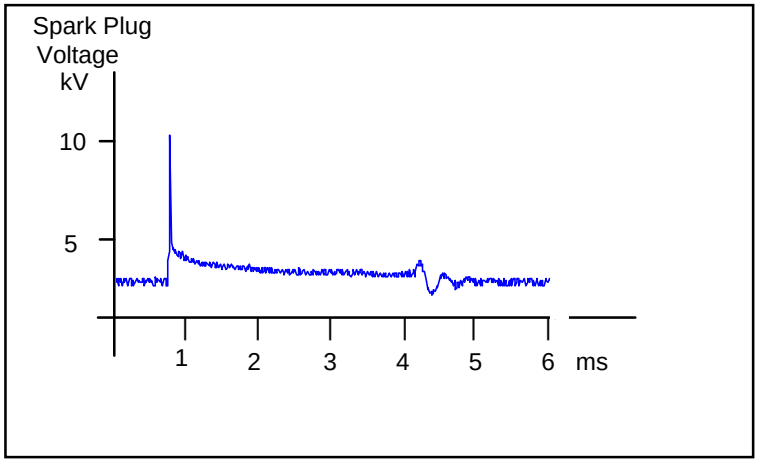

Figure 3. A typical spark voltage waveform.

Empirical observation of the spark plug voltage characteristic has shown that variations in engine parameters lead to changes in the shape of the voltage characteristic. It is predictable that the time-varying voltage exhibits certain major features, for example, a large peak early in the waveform. However, it is not easy to predict the detailed variations that occur as the engine parameters are varied. The signal-to-noise ratio is poor and random variations occur between sparks even when the operating parameters of the engine are kept constant.

The breakdown voltage across the electrode-gap of a spark plug in an operating IC engine is dependent on the interactions of many parameters, for example, the combustion chamber and electrode temperatures, the compression pressure, the electrode material and configuration, and the composition of the air-fuel gas mixture [10], [11]. All of these factors may be attributed to physical properties and processes; for example, the composition of the air-fuel mixture influences the breakdown voltage mainly through temperature and pressure changes.

The spark plug cathode electrode temperature has a significant effect on breakdown voltage, due to increased electron emission at elevated temperatures. The maximum spark plug temperature, when keeping other parameters constant, is achieved when the lambda-ratio is equal to 0.9, that is, the value for maximum power output. Under lean, and to a lesser extent, rich mixture conditions, the voltage rises; this is largely due to a reduction in the heat released by combustion. Given a constant set of engine operating conditions, an increase in lambda-ratio results in an increased pressure at ignition. This has been attributed to an increase in the ratio of specific heats (the gamma-ratio) of the air-fuel mixture; an increase in gas pressure results in a consequent rise in breakdown voltage [10]-[12].

Changes in lambda-ratio, and therefore in breakdown voltage, lead to subtle changes in the overall shape of the ignition spark waveform. Given a constant ignition system energy, an increase in breakdown voltage results in more energy being used within the breakdown phase. This leaves less energy available for following phases of the spark, i.e., the arc and glow discharge phases. The observed result is a reduction in the glow-discharge duration.

However, factors other than change in lambda are also likely to have an effect on the spark-voltage characteristic. For example, the temperature and pressure inside the cylinder, both of which are related to load, are relevant. In addition, the speed of the engine will determine the degree of in-cylinder turbulence which will also have an effect. Thus, if the voltage characteristic of the spark is to be used to determine the lambda-value, the effects of other parameters also must be accommodated.

To summarize, changes in the value of the lambda-ratio would be expected to influence both the breakdown voltage and the time-varying voltage characteristic of the arc and glow discharge phases. A formal relationship between the value of lambda and the instantaneous voltage at any particular point on the spark-voltage characteristic is not easily discernible and may not exist. However, theoretical considerations indicate a possible correlation between the vector formed by periodic sampling of the voltage at the spark plug over the spark time, termed the *spark-voltage vector*, and the lambda-ratio. With suitable pre-processing and training, a neural network is a suitable tool for associating the spark-voltage vector and lambda-ratio. This forms the basis of the Spark Voltage Characterization technique.

7 Neural Networks for Use in Virtual Sensors

Neural networks possess a number of specific qualities which make them invaluable in pattern-recognition applications and which are not easily achieved by other means. Some of the important qualities of neural networks can be summarized as follows:

- They learn by example and can be conditioned to respond correctly to a stimulus.
- They can automatically perform knowledge abstraction and statistical analyses on data which is presented to them and this information becomes encoded into the internal structure of the network.

- They can generalize so as to respond correctly even in the presence of noise or uncertainty making them suitable for use in poor signal-to-noise environments.

The use of neural networks for application to IC engine sensing [3], [13], [14], diagnostic monitoring [14]-[17] and control [18]-[20] is described in the literature, and new papers appear with increasing frequency. The contribution that neural networks can make in this area may be summarized as follows:

- Neural networks can interpret sensory data which is already present, or available at low cost, so as to extract new information.
- Neural networks can be used for the detection of specific *signatures* from new or existing sensors in OBD systems, in order to detect and identify fault conditions.
- Neural networks, and the related technology, *fuzzy systems*, can be valuable in achieving the non-linear mappings necessary for efficient engine-modeling and the implementation of advanced control strategies.

The SVC method makes use of the pattern-recognition abilities of the neural network for the interpretation of spark voltage vectors. The function of the neural network in this application was to categorize voltage vectors presented to it, differentiating between vectors corresponding to different values of lambda. Certain types of neural network are known to possess useful properties in this area, for example, the multi-layer perceptron (MLP). The MLP is essentially a static network, but it is routinely adapted to process dynamic data by the addition of a tapped delay-line. The delay-line is implemented algorithmically in software, forming the Time-Delay Neural Network [21]. It may be considered that the MLP projects n-element vectors, applied to it as inputs, into n-dimensional input space. Vectors belonging to different classes occupy different regions of this input-space. During the back-propagation learning or training process, a training-file containing exemplar vectors is repeatedly presented to the MLP, and it iteratively places hyper-plane partitions in such positions as to separate the classes attributed to the vectors. During the recall or the operational phase, a vector to be classified is presented to the MLP,

which categorizes it by determining where the vector lies in n-dimensional space in relation to the hyper-planes [22].

Feed-forward networks with sigmoidal non-linearities, such as the MLP, are very popular in the literature; however, networks which incorporate radially symmetric processing elements are more appropriate for certain classification applications. The Radial Basis Function (RBF) network is a neural classifier devised in its original form by Moody and Darken [23], but developed and enhanced by others [24]. Usually, the hidden layer consists of elements which perform Euclidean distance calculations, each being followed by a Gaussian activation function. A clustering algorithm is used to calculate the appropriate placings for the cluster centers; for example the k-means algorithm is widely used. In its most elementary form the output layer performs a linear summation of the non-linear outputs of the basis function elements. Alternatively, there can be advantages in the use of the basis neurons as a pre-processing layer for a conventional multi-layer feed-forward neural network, for example an MLP. The non-linear transformation effected by the basis neurons can be considered to move input-vectors into a space of a higher dimension. In some circumstances, the vectors are more easily separated in this higher-dimension space, than in space of their intrinsic dimension. In cases where the topology of the input-space is amenable, the use of RBF networks can lead to improved classification ability; benefits can also accrue in terms of shortened convergence times [24].

The neural network architecture best suited to a particular application depends largely on the topology of the input space (and, of course, on the criteria chosen for the comparison). However, the two network paradigms can be briefly compared as follows:

- The MLP achieves a concise division of the input space, with unbounded or open decision regions, using a comparatively small number of hidden neurons. The RBF network forms bounded or closed decision regions, using a much larger number of pattern (hidden) nodes, to provide a more detailed division of the input space.
- The MLP generally attains a higher classification speed, in its operational or recall mode, than a functionally comparable RBF

network. This is due to the more compact representation, which requires fewer hidden neurons.

8 AFR Estimation using Neural Network Spark Voltage Characterization

Here, a Virtual Lambda Sensor for the estimation of in-cylinder air-fuel ratio is described. The system exhibited a similar level of functionality to the conventional lambda sensor, which determines whether the air-fuel ratio is rich, correct or weak. However, the Virtual Lambda Sensor exhibited the advantage that no dedicated hardware sensor was required.

8.1 The Spark Voltage Characterization Method

The Virtual Lambda Sensor employed the spark voltage characterization method. The correlation between the spark-voltage vector and the lambda-ratio, discussed in Section 6, was exploited by training a neural network to associate specific spark voltage vectors with lambda-values. After training, the neural network was able to determine whether the lambda was correct, rich or weak, when it was presented with a spark voltage vector obtained from the engine operating with that mixture strength. It is recognized that factors other than the lambda would also have an effect on the spark-voltage vector, for example, changes in speed, load, etc. However, initially, the effect of these other parameters was ignored, and experiments were conducted under conditions where only the lambda was varied and other parameters were held constant. Later phases of the work will be concerned with accommodating changes in these other engine parameters.

Two stages in the investigation are presented. Firstly, experimental work using a multi-cylinder engine is described. A number of practical problems are identified, which lead to the second stage of the investigation, where a single-cylinder engine is used.

8.2 Neural Network Training Procedure

Figure 4 shows the experimental arrangement that was used. The engine was equipped with a dynamometer which presented the engine with a "dummy" load that could be varied as desired. The resulting load-torque could be measured and the output power calculated. The throttle setting and air-fuel ratio could be manually adjusted. The air-fuel ratio that resulted from this adjustment was measured by an exhaust gas analyzer. The ignition-system was modified by the addition of a high-voltage test-probe at the spark plug to enable the voltage to be measured and recorded.

A current transformer was fitted to the high-tension line to permit the recording of current data. However, no benefit was obtained from the use of current data and so results are not described.

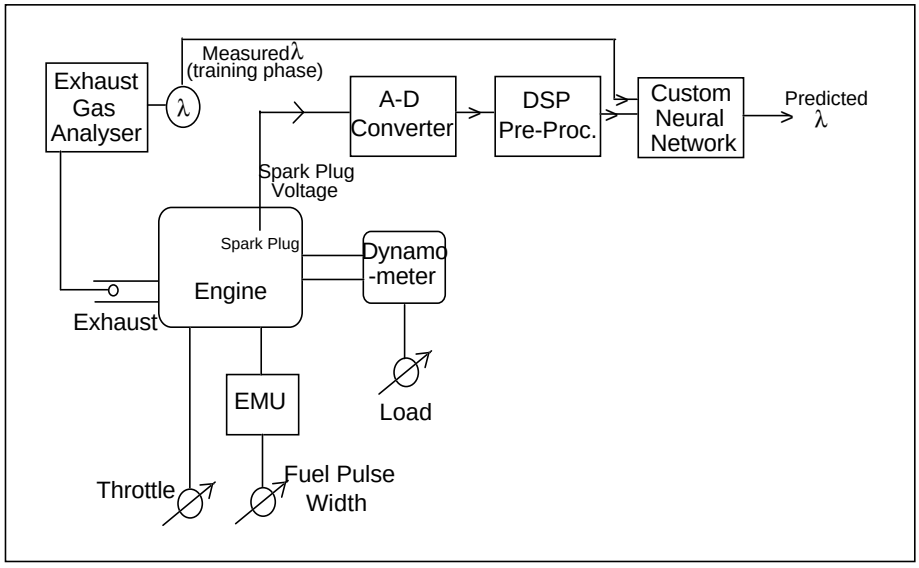

Figure 4. Spark voltage waveform capture system.

An MLP network, with a single hidden layer, and sigmoidal activation units, was used as a spark-voltage vector classifier. The architecture is illustrated in Figure 5. The backpropagation learning algorithm was applied to the MLP during training, which is a supervised training paradigm. This required that the training-file contain spark-voltage vectors, and desired-output vectors. The fuel pulse width and

dynamometer were adjusted to give an engine speed and a lambda-ratio of the desired values. Instantaneous spark-voltage vectors of the form $V_n = (v_1, v_2,\ldots,v_n)$ were created by recording the voltage at the spark plug at measured intervals of time. Each spark-voltage vector was associated with a desired-output vector, $D_r = (0,0,1)$, $D_c = (0,1,0)$, and $D_w = (1,0,0)$, depending on whether the lambda-value, measured by the exhaust gas analyzer, was rich, correct or weak, respectively. Three sets of spark-voltage vectors and their associated desired-output vectors were obtained, S_r, S_c and S_w, corresponding to rich, correct and weak lambda values. These vectors were combined into a single training-file, $F = \{S_r \cup S_c \cup S_w\}$. Similar files, having the same construction, but using data that was not used for training, were created for test purposes.

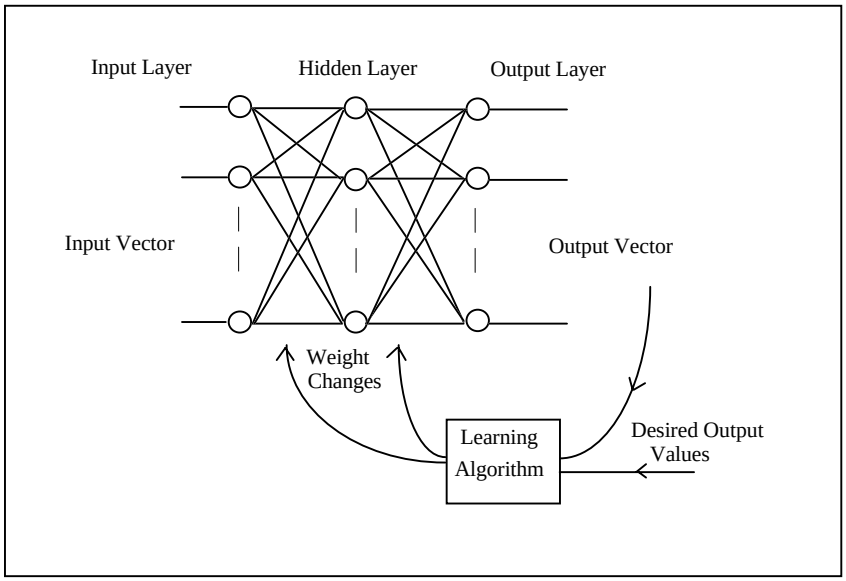

Figure 5. The architecture of the MLP neural network.

The MLP neural network was trained using cumulative back-propagation. The criterion used to determine when the training process should be terminated was based on ensuring that all neuron output values matched the corresponding desired-output value to within a selected convergence threshold T_c. For example, at the termination of the learning phase, the output of the jth output neuron is $y_j \geq 1 - T_c \;\forall\; v_n \in S_j$ and $y_j \leq T_c \;\forall\; v_m \in S_i \;(i = 1,\ldots r)\; i \neq j$.

8.3 The Multi-Cylinder Engine

An engine test-bed was used that was based on a 1400cc four-cylinder petrol-fueled spark-ignition engine of the type used in many domestic motor-cars. The experiments were conducted at a fixed engine speed of 1500 rpm, with an ignition-timing of 10 degrees before TDC and a wide-open throttle. Stoichiometric, lean and very lean air-fuel ratios were used which corresponded to lambda-ratios of 1.0, 1.2 and 1.4. These values of AFR produced output-torque values of 98.5, 85.0 and 62.8 Nm respectively.

8.3.1 Equal Sample Intervals

Three sets of training-files were constructed. Voltage data were recorded over the full duration of the spark using a fixed sampling interval for each file. The sampling intervals which were used for the three files were 10 μs, 20 μs and 40 μs respectively. Similar files were constructed for testing, using data which was not used for training. An MLP neural network, which executed a custom C-language implementation of the cumulative back-propagation algorithm, was trained using this data. In recall, the test-files were applied to the trained MLP network, where the output of the neural network was modified by a layer which executed a winner-takes-all paradigm. Table 1 shows the performance of the system under these conditions.

Table 1. Correct classification rate for various sampling intervals: single sampling interval.

Sampling Interval (μs)	40	20	10
Correct Classification Rate (%)	71	75	74

8.3.2 Unequal Sample Intervals

A second set of measurements was made with emphasis given to the peak region of the spark by using an increased sampling rate during the peak region compared to that used during tail times. The aim was to capture important transient variations in this region. Three training-files were constructed. Instantaneous voltage measurements were recorded

every 2 μs over the peak region for all three files, and then different sampling intervals of 10 μs, 20 μs and 40 μs were used for each file during the remainder of the spark duration. Table 2 shows the results.

Table 2. Correct classification rate for various sampling intervals; peak region emphasized.

Sampling Interval (μs)	40	20	10
Correct Classification Rate (%)	84	80	82

8.3.3 Integration of Instantaneous Values

In an attempt to reduce the effect of the random variations which were observed in successive spark waveforms, integration of instantaneous voltage values over a number of cycles was performed. Different sampling intervals were used during the peak and tail times, as described in Section 8.3.2, and different scale-factors were applied over the two regions. An MLP network was trained using training data which had been pre-processed in this way and a comparison was made using different sizes of training file. The network was trained using files containing 45, 60 and 75 training records, and tested in recall using 45 training records which had not been used in training. Table 3 shows the results that were obtained.

Table 3. Correct classification rate for various numbers of training sets : data integration used and peak region emphasized.

No Training Records	45	60	75
Correct Classification Rate (%)	86	87	93

8.3.4 Radial Basis Functions

In order to investigate whether the use of RBF elements would enhance the classification rate, the data used in Section 8.3.3 were applied to an RBF pre-processing layer, the outputs of which fed an MLP network.

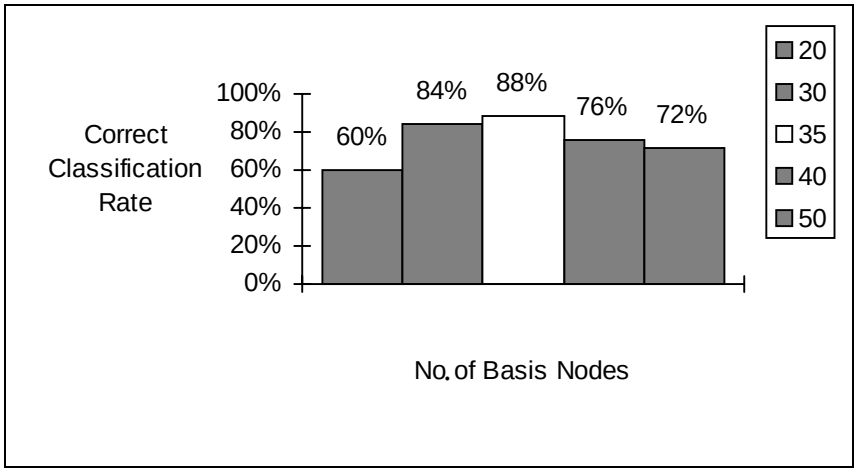

Figure 6. Graph showing correct classification rate for various numbers of hidden/basis nodes: peak region emphasized.

A version of the k-means clustering algorithm, which used semi-supervised learning, was applied to the RBF layer during training. The results which were obtained during recall, when varying numbers of basis nodes were used, are illustrated in Figure 6.

8.3.5 Discussion

Table 1 shows that the neural network could differentiate between the different classes of lambda on the basis of the spark voltage vector with a correct classification rate of between approximately 71 and 75%. With peak region emphasis, an improvement was obtained, as illustrated in Table 2, which shows a correct classification rate of between 80 and 84%. One interpretation of these results is that there was increased information available in the peak region of the spark. As the sampling interval was varied between 10 μs and 40 μs, no significant corresponding variation in classification rate was observed. The results presented in Table 3 show two things: firstly, an improvement in classification rate was observed when integration of instantaneous values was implemented; secondly, further improvements were obtained as the size of the training file was increased. The best classification rate that was obtained under these circumstances was 93%. The best classification rate obtainable using the RBF network was 88%, which was worse than the best rate obtained using the MLP network.

Inspection of the spark waveforms showed that random variations in the shape of successive spark-voltage vectors occurred even when engine parameters were kept as close to constant as practicably possible. The effect could be reduced by the use of integration over successive engine-cycles, as shown by improved results in Table 3. However, this could be an obstacle to the use of this technique for cycle-by-cycle lambda measurement, which is what is ultimately desired.

Observation of the output of the exhaust-gas analyzer showed that there were wide short-term variations in the lambda-ratio, even when the engine parameters were kept as constant as practically possible. These variations could be inherent to engine cyclic variations. A contributory factor could also be that the lambda value that was measured using the exhaust-gas analyzer was an average of the lambda in all four cylinders of the engine. The lambda-value in each cylinder was unlikely to be the same. The recorded spark-voltage vectors were those from only one of these four cylinders. The correlation between the spark-voltage vector obtained from one cylinder and the mean of the lambda-values in all four cylinders was likely to be poor.

The results in Table 3 indicated that better classification was obtained as the size of the training-file increased. However, the inherent instability of the engine made it impossible to maintain constant conditions for the time necessary to collect the required amount of training data.

8.4 The Single-Cylinder Engine

A single-cylinder engine offered a number of advantages over a multi-cylinder power unit. The correlation between the spark voltage vector, measured at the only spark plug of the single cylinder engine, and the lambda measured via the exhaust, was likely to be better than was obtainable in a multi-cylinder unit. The single-cylinder engine would also be likely to offer inherently increased lambda stability, allowing the capture of larger quantities of consistent data, which was required for improved classification.

The experimental arrangement that was used was similar to that shown in Figure 4, the power unit being a single-cylinder four-stroke engine

that had a capacity of 98.2cc. The engine was modified to enable manual adjustment to be made to the air-fuel ratio. This was measured using the same exhaust gas composition analyzer as had been used before. The ignition timing was fixed at 24 degrees before top-dead-center. A regenerative electric dynamometer was installed which allowed the load torque to be adjusted to a desired value.

8.4.1 Single-Speed Test

A fixed engine speed of 2800 rpm was selected. Rich, stoichiometric and lean air-fuel ratios were used which corresponded to lambda-ratios of 0.8, 1.0 and 1.2. These values were different to those selected for the multi-cylinder engine, because of the different characteristics of the two power units, but comparable for the purpose of this experiment. The experimental procedure that was described in Section 8.2 was followed. The MLP neural network was trained using a training-file composed of spark-voltage vectors and desired-output vectors. In recall, unseen training data were used. Experiments were conducted with a range of sample intervals. Under these circumstances the neural network virtual-sensor was able to determine the correct lambda-value, 0.8, 1.0 or 1.2 with a correct classification rate of approximately 100%. This performance was superior to that obtained with the multi-cylinder engine, where the best classification rate obtained was 93% (Table 3).

8.4.2 Multi-Speed Tests

A more comprehensive set of tests was carried out on the single-cylinder engine using a more closely spaced range of lambda values, i.e., 0.9, 1.0 and 1.1. A range of speeds and training file sizes was also used. Spark-voltage vectors and desired-output vectors were recorded at speeds of 2800 rpm, 3500 rpm and 4200 rpm. These speed-values corresponded approximately to the lower, middle and upper regions of the working speed range of the engine. Integration over a number of successive cycles was used to reduce the effects of random variations. Three training-files were created, one for each speed. Three similar files, containing data that was not used during training, were constructed for test purposes.

In order to investigate the effects of different numbers of training records, training-files of a number of different sizes were constructed.

The number of records (input-output vector pairs) in the training-file of an MLP network which leads to optimum classification has been the subject of much investigation; however, it has not proved amenable to formal analysis. Investigations described in the literature have indicated that a number of training-records comparable with, or exceeding, the number of weights in the network would lead to good classification ability over a representatively large body of test data. If an MLP network has P, Q and R neurons in the input, hidden and output layers, respectively, the number of weights in the network, N_w, equals $(P + 1)Q + (Q + 1)R$. Letting the number of records in the training file be N_t, then $N_t = \sigma \cdot N_w$ where σ is the *normalized size* of the training file, and $1 < \sigma < 10$ for good classification performance. The optimum value of σ depends on the shape of the P-dimensional feature space, which is, in turn, determined by the problem domain. Generally, large values of σ lead to better classification and generalization; however, adoption of this criterion often leads to a large training-file size and an extended time requirement for network convergence.

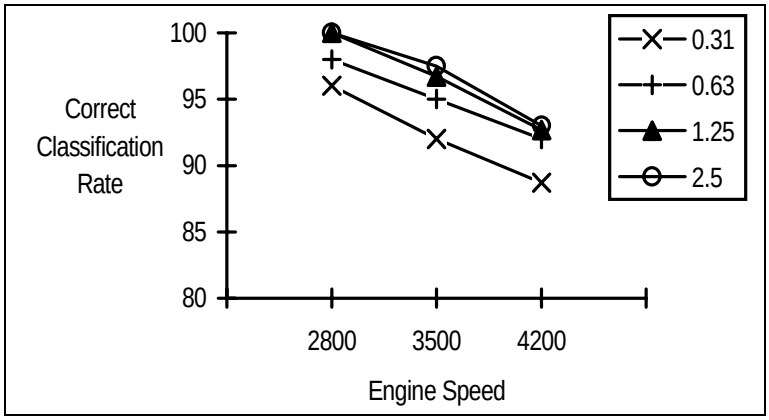

Figure 7. Correct classification rate against engine speed for various normalized training file sizes.

Figure 7 shows the classification performance which was obtained at different speeds and for different values of σ. At 2800 rpm the neural network virtual-sensor could determine the lambda-ratio with a correct classification rate of approximately 100% when either of the largest two file sizes were used during training. Smaller training file sizes resulted in poorer classification rates. At higher speeds the classification rate was not as good. Increasing the size of the training file resulted in an

improvement in performance to an extent; however, only a small improvement was evident as the σ is increased from 1.25 to 2.5. This suggested that the decrease in classification ability was due to some inherent change in input data as the speed was increased.

No conclusive reason has been found for the decrease in classification rate with speed and this phenomenon requires further investigation. There are two suggested possible reasons:

- Increased instability in the engine as the speed is increased could result in wider variations in the actual lambda-value about the nominal value. If this was so the signal-to-noise ratio of the data would effectively increase with the speed. This would impair the ability of the neural network to correctly categorize the spark voltage vectors.
- The same sample rate was used for all speeds. At higher speeds fewer measurements were made per revolution. It is possible that the reduced classification rate at higher speeds was due to the worsening of the sampling resolution caused by this.

9 Conclusions

A Virtual Lambda Sensor, using the Spark Voltage Characterization technique, has been introduced here. The system implements neural network analysis of the spark-voltage vector, in order to provide an estimate of the in-cylinder air-fuel ratio. The experimental work shows that the virtual-sensor can provide analogous functionality to the conventional lambda-sensor, but without the need for the usual hardware sensor. The Virtual Lambda Sensor is capable of determining when the lambda-ratio is stoichiometric, or when it deviates from this value by approximately ±10% (*lambda* = 1.0 ± 0.1), with the engine operating under fixed speed and load conditions.

A description has been given of the relatively early stages of the development of the technique. To be practicable as a replacement for the conventional lambda-sensor in a commercial engine, improvements to the Virtual Lambda Sensor are necessary in two respects: firstly, the accuracy of the estimation must be improved, 1% is an aim imposed by

the catalytic converter; and secondly, variations in speed, load, etc., must be accommodated.

Improved accuracy demands that the neural network is trained with lambda data which is of higher consistency. Although quantitative measurements are not presented here, observation of the output voltage from the exhaust-gas analyzer using an oscilloscope showed that the lambda-value, under constant engine conditions, could vary from its nominal value by up to approximately 7%. The accuracy which has been achieved is probably close to the best achievable using the current methodology. However, initial results obtained using a more sophisticated experimental methodology have demonstrated improved accuracy.

A mechanism for dealing with variations in speed, load, etc., is the creation of overlays to the neural network weight-matrix for different physical conditions. However, this is likely to impose a large training time penalty. Mathematical analysis of the dynamic physical system is also being implemented to provide guidance about the optimum pre-processing of the data before it is used in the neural network training phase.

Acknowledgment

This work was carried out at the ***Transfrontier Centre for Automotive Research*** **(TCAR)** which is financially supported by the European Union under the Interreg II Programme of the European Regional Development Fund, grant number ES/B3/01.

References

[1] Kimberley, W. (1997), "Focus on emissions," *Automotive Engineer,* Vol. 22, No.7, pp. 50-64.

[2] Boam, D.J., Finlay, I.C., Biddulph, T.W., Ma, T.A., Lee, R., Richardson, S.H., Bloomfield, J., Green, J.A., Wallace, S., Woods, W.A. and Brown, P. (1994), "The sources of unburnt hydrocarbon emissions from spark ignition engines during cold starts and warm-up," *Proceedings of The Institution of Mechanical Engineers. Journal of Automobile Engineering, Part D*, 208, pp. 1-11.

[3] Atkinson, C.M., Long, T.W. and Hanzevack, E.L. (1998), "Virtual sensing: a neural network-based intelligent performance and emissions prediction system for on-board diagnostics and engine control," *Proceedings of the 1998 SAE International Congress & Exposition*, vol. 1357, pp. 39-51.

[4] Cardini, P. (1999), "Focus on emissions: going for the burn," *Automotive Engineer*, vol. 24, no. 8, pp. 48-52.

[5] Eriksson, L. and Nielsen, L. (1997), "Ionization current interpretation for ignition control in internal combustion engines," *Control Engineering Practice*, vol. 5, no 8, pp. 1107-1113.

[6] Balles, E.N., VanDyne, E.A., Wahl, A.M., Ratton, K. and Lai, M.C. (1998), "In-cylinder air/fuel ratio approximation using spark gap ionization sensing," *Proceedings of the 1998 SAE International Congress & Exposition*, vol. 1356, pp. 39-44.

[7] Ohashi, Y., Fukui, W., Tanabe, F. and Ueda, A. (1998), "The application of ionic current detection system for the combustion limit control," *Proceedings of the 1998 SAE International Congress & Exposition*, vol. 1356, pp. 79-85.

[8] Hellring, M., Munther, T., Rognvaldsson, T., Wickstrom, N., Carlsson, C., Larsson, M., and Nytomt, J. (1998), "Spark Advance Control using the Ion Current and Neural Soft Sensors," *SAE Paper 99P-78*.

[9] Hellring, M., Munther, T., Rognvaldsson, T., Wickstrom, N., Carlsson, C., Larsson, M. and Nytomt, J. (1998), "Robust AFR estimation using the ion current and neural networks," *SAE Paper 99P-76*.

[10] Champion Spark Plugs. (1987), *Straight Talk About Spark Plugs*.

[11] NGK Spark Plug Co. Ltd. (1991), *Engineering Manual For Spark Plugs*, OP-0076-9105.

[12] Pashley, N.C. (1997), *Ignition Systems For Lean-burn Gas Engines*, Ph.D. Thesis, Department of Engineering Science, University of Oxford, U.K.

[13] Frith, A.M., Gent, C.R. and Beaumont, A.J. (1995), "Adaptive control of gasoline engine air-fuel ratio using artificial neural networks," *Proceedings of the Fourth International Conference on Artificial Neural Networks*, no. 409, pp. 274-278.

[14] Ayeb, M., Lichtenthaler, D., Winsel, T. and Theuerkauf, H.J. (1998), "SI engine modeling using neural networks," *Proceedings of the 1998 SAE International Congress & Exposition*, vol. 1357, pp. 107-115.

[15] Wu, Z.J. and Lee, A. (1998), "Misfire detection using a dynamic neural network with output feedback," *Proceedings of the 1998 SAE International Congress & Exposition*, vol. 1357, pp. 33-37.

[16] Ribbens, W.B., Park, J., and Kim, D. (1994), "Application of neural networks to detecting misfire in automotive engines," *IEEE International Conference on Acoustics, Speech and Signal Processing*, vol. 2, pp. 593-596.

[17] Ortmann, S., Rychetsky, M., Glesner, M., Groppo, R., Tubetti, P. and Morra, G. (1998), "Engine knock estimation using neural networks based on a real-world database," *Proceedings of the 1998 SAE International Congress & Exposition*, vol. 1357, pp. 17-24.

[18] Muller, R. and Hemberger, H.H. (1998), "Neural adaptive ignition control," *Proceedings of the 1998 SAE International Congress & Exposition*, vol. 1356, pp. 97-102.

[19] Lenz, U. and Schroder, D. (1998), "Air-fuel ratio control for direct injecting combustion engines using neural networks," *Proceedings of the 1998 SAE International Congress & Exposition*, vol. 1356, pp. 117-123.

[20] Baumann, B., Rizzoni, G. and Washington, G. (1998), "Intelligent control of hybrid vehicles using neural networks and fuzzy logic," *Proceedings of the 1998 SAE International Congress & Exposition*, vol. 1356, pp. 125-133.

[21] Hush, D.R. and Horne, B.G. (1993), "Progress in supervised neural networks," *IEEE Signal Processing Magazine*, pp. 8-39.

[22] Hush, D.R., Horne, B. and Salas, J.M. (1992), "Error surfaces for multilayer perceptrons," *IEEE Transactions on Systems, Man and Cybernetics*, vol.22, no.5, pp.1152-1161.

[23] Moody, J. and Darken, C.J. (1989), "Fast learning in networks of locally tuned processing units," *Neural Computation*, vol.1, pp. 281-294.

[24] Leonard, J.A., Kramer, M.A. and Ungar, L.H. (1992), "Using radial basis functions to approximate a function and its error bounds" *IEEE Transactions on Neural Networks*, vol.3, no.4, pp. 625-627.

[25] Fu, L. (1994), *Neural Networks in Computer Intelligence*, McGraw-Hill, New York.